R. S. Jangid
Department of Civil Engineering
Indian Institute of Technology
Powai, Bombay 400 076, India

T. K. Datta
Department of Civil Engineering
Indian Institute of Technology
Hauzkhas, New Delhi 110 016, India

Dissipation of Hysteretic Energy in Base Isolated Structure

Dissipation of hysteretic energy in the isolator of the base isolated structure under seismic excitation is investigated. The hysteretic force-deformation characteristics of the base isolator is specified by a nonlinear differential equation. The parameters of the equation can be adjusted to obtain various types of hysteretic models of the isolator including the elastoplastic type. The variation of hysteretic energy dissipated in the isolators is obtained for both harmonic and El-Centro 1940 earthquake ground motion for a set of important parameters. They include time period of superstructure, ratio of superstructure mass to base mass, level of yield strength of the isolator, post- to preyielding stiffness ratio, and the ratio of harmonic excitation frequency to base isolation frequency. It is shown that the dissipation of hysteretic energy in the isolator is significantly influenced by the above parameters. © *1996 John Wiley & Sons, Inc.*

INTRODUCTION

The traditional method of providing earthquake resistance to a structure is by increasing its strength as well as energy absorbing capacity. However, during an earthquake many structures have suffered structural and nonstructural damages due to inelastic deformations. An alternative method is to isolate the structure by the use of base isolators between the base of the structure and its foundation. These base isolators have two important characteristics: horizontal flexibility and energy absorbing capacity. Horizontal flexibility lowers the fundamental frequency of the structure below the range of frequencies that dominate in general earthquake excitation. Energy absorbing capacity reduces both relative displacements and seismic energy being transmitted to the structure. The effectiveness of various types of base isolation in limiting the earthquake forces in buildings was demonstrated (Constantinou and Tadjbakhsh, 1985; Fan and Ahmadi, 1990). An excellent review for the earlier works and recent investigations on base isolation was provided by Buckle and Mayes (1990) and Jangid and Datta (1995).

A variety of base isolation devices including laminated rubber bearings (LRBs), frictional bearings, and roller bearings have been developed. The LRBs are one of the most commonly used bearings. Recently, friction-type base isolators have been developed and studied. The most attractive feature of this type of isolator is that the friction force is a natural and powerful energy-dissipation device. The simplest such device is pure friction, referred to as the P-F system or sliding-type structure (Ahmadi, 1981; Mostaghel and Tanbackuchi, 1983). The more advanced devices involve pure-friction elements in combination with LRB (Mostaghel and Khodaverdian,

Received December 6, 1994; Accepted March 4, 1996.
Shock and Vibration, Vol. 3, No. 5, pp. 353–359 (1996)

CCC 1070-9622/96/050353-07

1987). A comparative study of the performance of different base isolation systems was carried out by several authors (Su et al., 1989; Lin et al., 1990). The LRB isolators, also called elastomeric bearings, could be of different types and may provide both linear and nonlinear force-deformation behavior (for example, New Zealand rubber bearing with lead core). In the former, seismic energy is absorbed by the viscous dampers provided along with the isolation device. In the latter, seismic energy is absorbed both by hysteretic force-deformation behavior of the isolator and by the additional viscous dampers. The control of seismic energy being transmitted to the superstructure is predominantly governed by hysteretic characteristics of the isolator. The response level of the superstructure is thus significantly influenced by the hysteretic loss of energy input. There have been several studies both experimental (Kelly and Beucke, 1983) and theoretical (Constantinou and Tadjbakhsh, 1985; Fan and Ahmadi, 1990; Jangid and Datta, 1994) on the response characteristics of the base isolated structures under important parametric variations. Comparatively less studies have been carried out in investigating the energy dissipated in isolators under different parametric variations. Such studies are important not only in understanding the behavior of isolators under cyclic loading, but also in its design for effective control of structural response.

Herein the response behavior of base isolated single-story shear-type buildings to harmonic and El-Centro 1940 earthquake ground motion is presented. The restoring force of the elastomeric bearing (isolator) is modeled by a nonlinear differential equation. The objectives of the study are: to study the effect of hysteretic energy dissipation on the effectiveness of base isolation; to investigate the effect of various important parameters on the hysteretic energy dissipation in the isolator; and to study the variation of the hysteretic energy dissipation of the base isolation system under different frequencies of excitation in comparison to the base isolation frequency.

STRUCTURAL MODEL

Figure 1 shows the structural system considered, which is an idealized one-story building model mounted on an elastomeric bearing. The rigid deck mass is supported by massless inextensible columns. The columns are assumed to remain

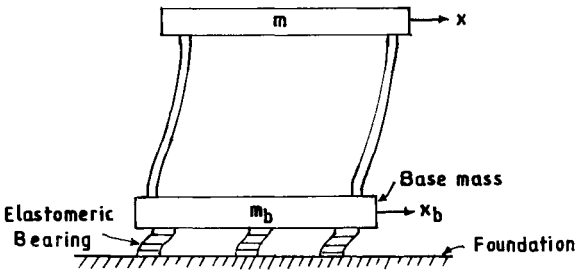

FIGURE 1 Structural model.

within the elastic range during the earthquake excitation. This is a reasonable assumption, because the purpose of base isolation is to reduce the earthquake effects in such a way that the structure remains within the elastic limits. The 2 degrees of freedom considered are lateral displacement of the deck (x) and lateral displacement of the base isolator (x_b). Further, the isolator is assumed to carry the vertical load without undergoing any vertical deformation. An additional damping C_b is assumed to be provided by the dampers. The force-deformation relationship of elastomeric bearings is mathematically idealized by an empirical equation suggested by Wen (1976). The restoring force, F_b, is given by the relation

$$F_b(x_b, \dot{x}_b) = \alpha k_b x_b + (1 - \alpha) k_b Z, \qquad (1)$$

in which x_b and $\dot{x}_b$ are the displacement and velocity in the elastomeric bearing, respectively; α is the post- to preyielding stiffness ratio; $k_b = Q_y/q$ is the initial stiffness of the elastomeric bearing; Q_y and q are the yield force and yield displacement of the elastomeric bearing, respectively; and Z is a dimensionless hysteretic displacement satisfying the following nonlinear first-order differential equation:

$$\frac{dZ}{dt} = -\beta|\dot{x}_b|Z|Z|^{n-1} - \tau\dot{x}|Z|^n + A\dot{x}_b, \qquad (2)$$

in which β, τ, n, and A are dimensionless parameters. The force-deformation behavior of the elastomeric bearing can be modeled by properly selecting the parameters Q_y, q, α, β, τ, n, and A. A typical smooth hysteresis loop of the elastomeric bearing using Eqs. (1) and (2) under sinusoidal displacement of amplitude of 0.1 m and frequency 1 Hz is shown in Fig. 2. The parameters are Q_y = 800 N, q = 0.025 m, α = 0 (elastoplastic), β = τ = $0.5q^2$, n = 2, and A = 1.

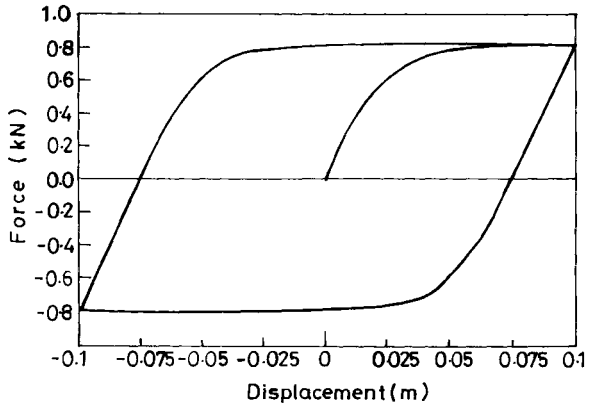

FIGURE 2 Force-deformation behavior of the isolator.

The rate of hysteretic energy dissipated in the elastomeric bearing at time t is given by

$$\frac{dE_h}{dt} = (1 - \alpha)k_b Z\dot{x}_b, \tag{3}$$

and the total hysteretic energy dissipated at time t is

$$E_h = (1 - \alpha)k_b \int_0^t Z\dot{x}_b d\tau. \tag{4}$$

EQUATIONS OF MOTION

The equations of motion for the system under consideration are

$$m\ddot{x} + c\dot{x} + kx = -m(\ddot{x}_b + \ddot{x}_g), \tag{5}$$

$$m_b\ddot{x}_b + c_b\dot{x}_b + F_b - c\dot{x} - kx = -m_b\ddot{x}_g, \tag{6}$$

in which, m, c, and k are the mass, damping, and stiffness of the superstructure; x is the displacement of the superstructure relative to base mass; m_b is the base mass; C_b is the viscous damping provided by the elastomeric bearings; F_b is the restoring force of the elastomeric bearings obtained from Eq. (1); x_b is the base displacement relative to ground; and $\ddot{x}_g$ is the ground acceleration.

INCREMENTAL SOLUTION PROCEDURE

Because the restoring force of the elastomeric bearing is a nonlinear function of displacement and velocity, the equations of motion are solved in the incremental form. The Newmark's β method is chosen for the solution of incremental differential equations, assuming the linear variation of acceleration over a small time interval, δt. Equations (5) and (6) can be written in the following incremental form:

$$m\delta\ddot{x} + c\delta\dot{x} + k\delta x = -m(\delta\ddot{x}_b + \delta\ddot{x}_g), \tag{7}$$

$$m_b\delta\ddot{x}_b + c_b\delta\dot{x}_b + \delta F_b - c\delta\dot{x} - k\delta x = -m_b\delta\ddot{x}_g. \tag{8}$$

The incremental force δF_b from Eq. (1) is expressed as

$$\delta F_b = \alpha k_b \delta_b + (1 - \alpha)k_b\delta Z. \tag{9}$$

Following the assumption of linear variation of acceleration over δt, the incremental acceleration and velocity of the superstructure are expressed as

$$\delta\ddot{x} = a_0\delta x + a_1\dot{x}^t + a_2\ddot{x}^t, \tag{10}$$

$$\delta\dot{x} = b_0\delta x + b_1\dot{x}^t + b_2\ddot{x}^t, \tag{11}$$

in which $a_0 = 6/\delta t^2$, $a_1 = -6/\delta t$, $a_2 = -3$, $b_0 = 3/\delta t$, $b_1 = -3$, and $b_2 = -\delta t/2$. The superscript t denotes the time. Similarly, the $\delta\ddot{x}_b$ and $\delta\dot{x}_b$ can be obtained by replacing x by x_b in Eqs. (10) and (11), respectively.

To solve the incremental equations, Eqs. (7)–(9) an iterative procedure is required, because computation of δF_b requires the knowledge of δZ that in turn depends upon the incremental displacement δx_b. In the iterative procedure the value of δZ at each time step is obtained by solving Eq. (2) with the help of the third-order Runge–Kutta method. The iteration starts with $\delta Z = 0$ and the δx and δx_b are then calculated using Eqs. (7)–(9). The velocity vector, $\dot{x}_b^{t+\delta t}$ is obtained as

$$\delta\dot{x}_b^{t+\delta t} = b_0\delta x_b + (b_1 + 1)\dot{x}_b^t + b_2\ddot{x}_b^t. \tag{12}$$

The revised value of the δZ is obtained by using the Runge–Kutta method as

$$\delta Z = \frac{K_0 + 3K_2}{4} \tag{13}$$

and

$$K_0 = \delta t g(\dot{x}_b^t, Z), \tag{14a}$$

$$K_1 = \delta t g(\dot{x}_b^{t+\delta t/3}, Z + K_0/3), \tag{14b}$$

$$K_2 = \delta t g(\dot{x}_b^{t+2\delta t/3}, Z + 2K_1/3). \tag{14c}$$

The function g in Eq. (14) denotes the right-hand side of Eq. (2). The iterations are continued until the convergence is achieved. The following convergence criteria is used.

$$\frac{\delta Z_{j+1} - \delta Z_j}{Z_m} \leq \varepsilon, \tag{15}$$

$$Z_m = \sqrt[n]{\frac{A}{\beta + \tau}}, \tag{16}$$

in which ε is the tolerance and Z_m is the maximum value of hysteretic displacement for elastoplastic (i.e., $\alpha = 0$) elastomeric bearings (Wen, 1976). The parameters A, β, τ, and n are defined in Eq. (2). The subscript to Z denotes the iteration number.

When the convergence criterion is satisfied, the incremental δx and δx_b are obtained from Eq. (11). The incremental restoring force δF_b is obtained from Eq. (9). The restoring force at time $t + \delta t$ is given by

$$F_b^{t+\delta t} = F_b^t + \delta F_b. \tag{17}$$

The acceleration x and x_b at time $t + \delta t$ are evaluated directly from the consideration of equilibrium, Eqs. (5) and (6), respectively. The incremental hysteretic energy dissipated is given by:

$$\delta E_h = \frac{L_0 + 3L_2}{4}, \tag{18}$$

where

$$L_0 = \delta t(1 - \alpha)k_b Z^t \dot{x}_b^t, \tag{19a}$$

$$L_1 = \delta t(1 - \alpha)k_b(Z^t + L_0/3)\dot{x}_b^{t+\delta t/3}, \tag{19b}$$

$$L_2 = \delta t(1 - \alpha)k_b(Z^t + 2L_1/3)\dot{x}_b^{t+2\delta t/3}. \tag{19c}$$

The hysteretic energy dissipated at time $t + \delta t$ is given by

$$E_h^{t+\delta t} = E_h^t + \delta E_h. \tag{20}$$

Response to El-Centro 1940 Earthquake Excitation

First, the response of the system was obtained from the N00W component of the El-Centro 1940 earthquake ground acceleration record. The response of the system was investigated for the variation of the following parameters: time period of the superstructure (T), the ratio of base mass to superstructure mass (m_b/m), level of yield strength of the elastomeric bearing (Q_y), and post- to preyielding stiffness ratio of the isolator (α). The specifications for the values of the parameters (held constant) were: total mass of the system, i.e., $m + m_b = W/g = 1000$ kg (W is the total weight of the structure and g is acceleration due to gravity); yield displacement, $q = 0.025$ m; $\beta = \tau = 0.5/q^2$; $n = 2$; $A = 1$; the modal damping for the superstructure is 5% of the critical; and the damping constant of the elastomeric bearing is taken as 0.1.

The time variation of normalized hysteretic energy dissipated for $\alpha = 0$, 0.25, and 0.5 is shown in Fig. 3. The dissipation of hysteretic energy increases with the increase of time. The dissipation of hysteretic energy is more for $\alpha = 0$ (i.e., elastoplastic elastomeric bearings).

The variation of hysteretic energy dissipated against the time period of the superstructure is shown in Fig. 4. The dissipation of hysteretic energy decreases with the increase of time period T. Further, the dissipation of hysteretic energy is more for $\alpha = 0$. Thus, the dissipation of hysteretic energy in the isolator decreases as the superstructure becomes flexible.

The variation of the response ratio R (the ratio of peak superstructure absolute acceleration of the base isolated system to the corresponding peak acceleration of the fixed base system) against the time period of the superstructure is shown in Fig. 5. The ratio R increases with the increase of the time period. This is expected because the capacity of the isolator to dissipate the seismic energy decreases as the time period of the superstructure decreases (Fig. 4); therefore,

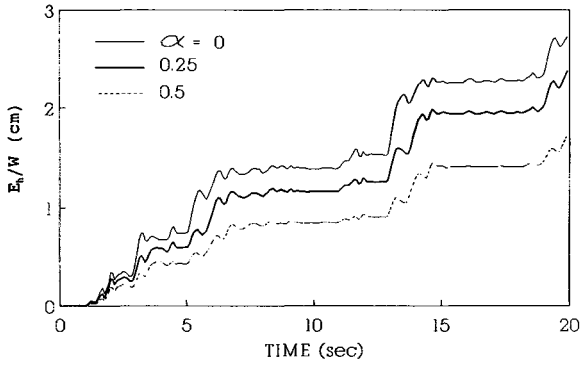

FIGURE 3 Time variation hysteretic energy dissipated for El-Centro earthquake: $T = 1$ s, $m_b/m = 1.5$, and $Q_y/W = 0.08$.

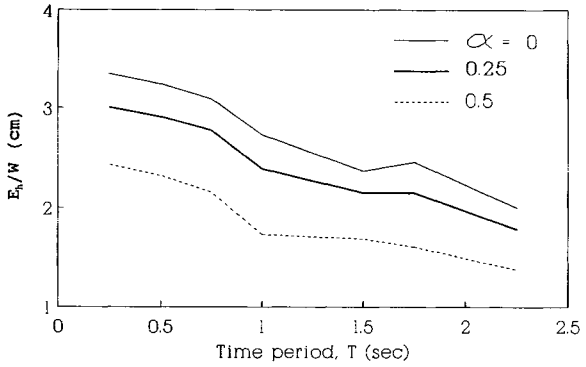

FIGURE 4 Variation of hysteretic energy dissipated against time period of superstructure; $m_b/m = 1.5$ and $Q_y/W = 0.08$.

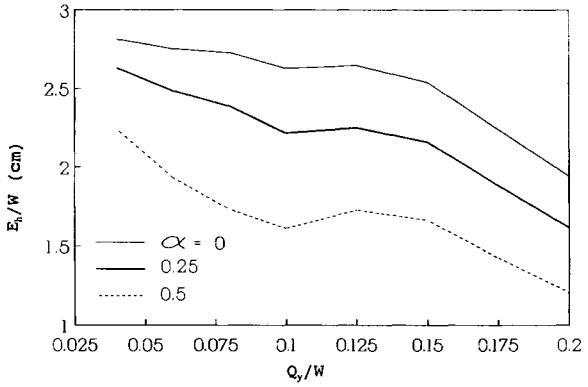

FIGURE 6 Variation of hysteretic energy dissipated against Q_y/W; $T = 1$ s and $m_b/m = 1.5$.

the effectiveness of the base isolation decreases. Thus, the dissipation of hysteretic energy controls the effectiveness of a base isolation system.

In Fig. 6 the variation of hysteretic energy dissipated is plotted against the level of the yield force of the isolator, Q_y. The dissipation of hysteretic energy decreases monotonically with the increase in Q_y/W up to a value of $Q_y/W = 0.1$. After that, there is a little increase in the hysteretic energy (up to $Q_y/W = 0.125$) and then it again starts to decrease. It generally shows higher dissipation of energy at a very low value of $Q_y(Q_y/W < 0.1)$. This is due to the fact that for low values of yield force, the system undergoes more cycles of the hysteresis loop; as a result, the hysteretic energy is dissipated more.

Variation of hysteretic energy dissipated with mass ratio m_b/m is shown in Fig. 7. It is observed from the figure that the dissipation of hysteretic energy is not significantly influenced by the mass ratio.

Response to Sinusoidal Excitation

The harmonic ground acceleration is expressed as

$$\ddot{x}_g = a \sin(\Omega t), \tag{21}$$

in which a is the amplitude and Ω is the frequency of excitation. For the present study, a was taken as $0.25g$. The effects of the parameters T, m_b/m, Q_y, α, and Ω/w_b were investigated. The w_b is the frequency of base isolation (i.e., $w_b = \sqrt{k_b/(m + m_b)}$. The values of the other parameters remained the same as those for the El-Centro earthquake excitation. The duration of the harmonic excitation was taken as 15 s.

The variation of hysteretic energy dissipation with frequency ratio, Ω/w_b for $\alpha = 0$, 0.25, and 0.5 is shown in Fig. 8. For $\alpha = 0.25$ and 0.5, it is sharply peaked; the peak is centered around the fundamental natural frequency of the isolated structure with isolator stiffness as αk_b. However,

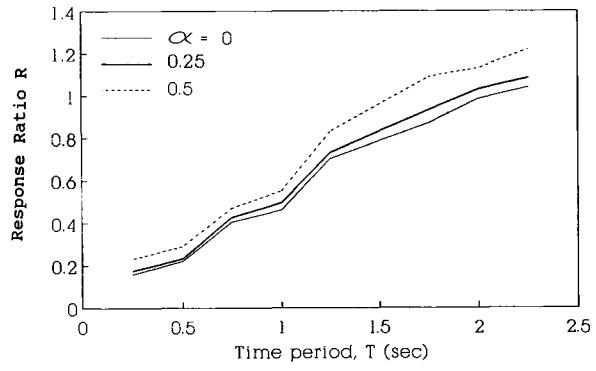

FIGURE 5 Variation of response ratio R against time period of superstructure; $m_b/m = 1.5$ and $Q_y/W = 0.08$.

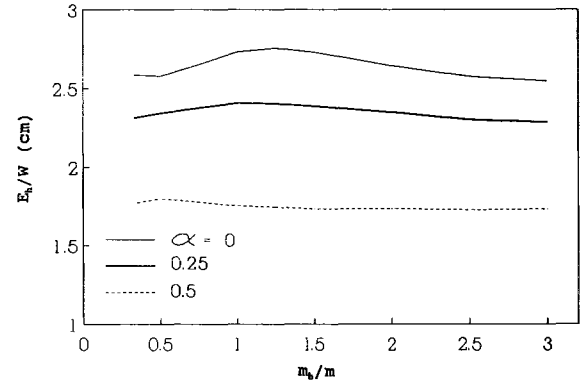

FIGURE 7 Plot of hysteretic energy dissipated against mass ratio m_b/m; $T = 1$ s and $Q_y/W = 0.08$.

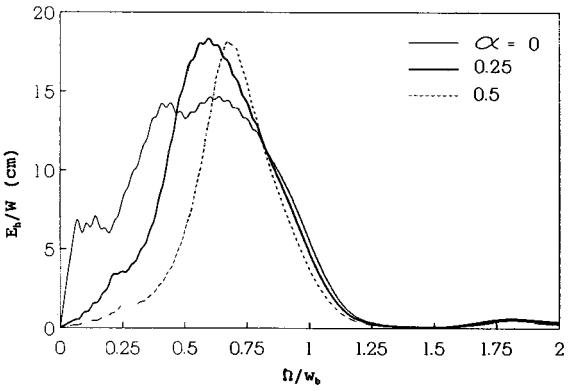

FIGURE 8 Variation hysteretic energy dissipated against harmonic frequency of excitation; $T = 1$ s, $m_b/m = 1.5$, and $Q_y/W = 0.08$.

for $\alpha = 0$ the variation is similar but there is no definite maxima. Further, for $\Omega/w_b > 1.25$, the dissipation of hysteretic energy is insensitive to the value of α. Thus, the dissipation of hysteretic energy is maximum for excitation frequencies in the vicinity of the natural frequency of the system (computed based on the postyield stiffness of the isolator).

The time variation of hysteretic energy dissipated for $\alpha = 0$, 0.25, and 0.5 is shown in Fig. 9. The harmonic excitation frequency is taken as $0.25w_b$. The dissipation of hysteretic energy increases with the increase of time. The dissipation of hysteretic energy is more for $\alpha = 0$ (i.e., elastoplastic).

The variation of hysteretic energy dissipated against T, Q_y, and m_b/m is shown in Figs. 10–12, respectively, for $\Omega/w_b = 0.25$. The trend of the variation of hysteretic energy dissipated remains the same as those observed for the El-Centro 1940 earthquake excitation.

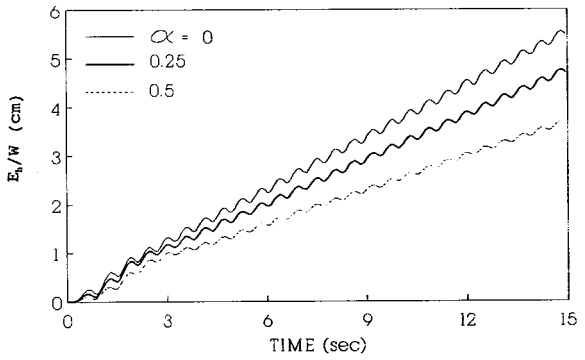

FIGURE 9 Time variation hysteretic energy dissipated for harmonic excitation; $T = 1$ s, $m_b/m = 1.5$, and $Q_y/W = 0.08$.

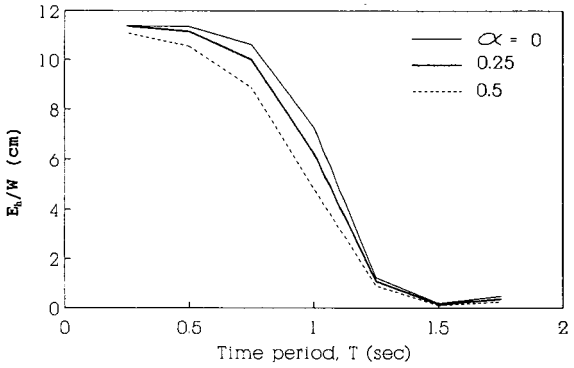

FIGURE 10 Variation of hysteretic energy dissipated against time period T; $m_b/m = 1.5$ and $Q_y/W = 0.08$.

CONCLUSIONS

The dissipation of hysteretic energy in the isolator of a one-story shear-type base isolated structure to both harmonic and El-Centro 1940 earthquake ground motion was studied. The effect of important parameters on the dissipation of hysteretic energy was investigated. The various conclusions derived from the results of the present study are:

1. The dissipation of hysteretic energy controls the effectiveness of a base isolation system. The effectiveness of the base isolation increases as the hysteretic energy dissipated in the isolator increases.
2. The dissipation of hysteretic energy in the isolator decreases as the superstructure becomes flexible.
3. The dissipation of hysteretic energy in the isolator of the base isolated structure decreases as the level of yield force increases.

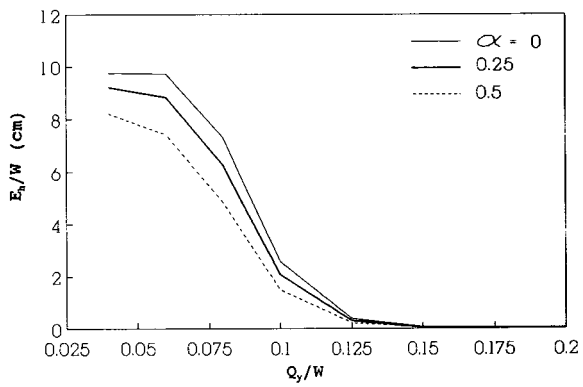

FIGURE 11 Variation of hysteretic energy dissipated against Q_y/W; $T = 1$ s and $m_b/m = 1.5$.

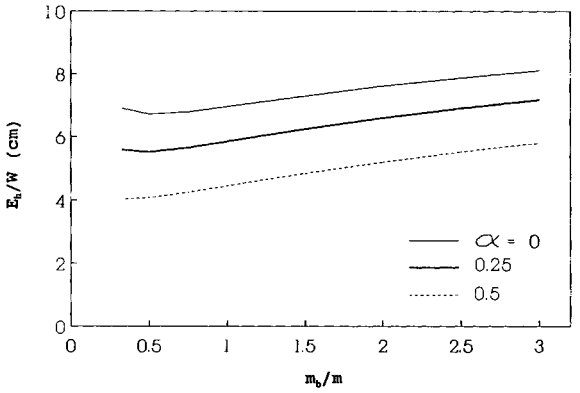

FIGURE 12 Plot of hysteretic energy dissipated against mass ratio m_b/m; $T = 1$ s and $Q_y/W = 0.08$.

4. The hysteretic energy dissipated is not significantly influenced by the ratio of base mass to superstructure mass.
5. The dissipation of hysteretic energy is maximum for the elastoplastic base isolation system. It decreases with the increase of post- to preyielding stiffness ratio.
6. The dissipation of hysteretic energy in the isolator is maximum for harmonic excitation frequencies in the vicinity of the natural frequency of the structure (computed based on the postyield stiffness of the isolator).

REFERENCES

Ahmadi, G., 1983, "Stochastic Earthquake Response of Structure on Sliding Foundation," *International Journal of Engineering Science,* Vol. 21, pp. 93–102.

Buckle, I. G., and Mayes, R. L., 1990, "Seismic Isolation: History, Application and Performance—A World Overview," *Earthquake Spectra,* Vol. 6, pp. 161–202.

Constantinou, M. C., and Tadjbakhsh, I. G., 1985, "Hysteretic Dampers in Base Isolation: Random Approach," *Journal of Structural Engineering, ASCE,* Vol. 111, pp. 705–721.

Fan, F., and Ahmadi, G., 1990, "Flood Response Spectra for Base-Isolated Multi-Storey Structures," *Earthquake Engineering and Structural Dynamics,* Vol. 19, pp. 377–388.

Jangid, R. S., and Datta, T. K., 1994, "Non-Linear Response of Torsionally Coupled Base Isolated Structure," *Journal of Structural Engineering, ASCE,* Vol. 120, pp. 1–22.

Jangid, R. S., and Datta, T. K., 1995, "Seismic Behaviour of Base Isolated Building—A-State-of-the-Art-Review," *Journal of Structures and Buildings, ICE,* Vol. 110, pp. 186–203.

Kelly, J. M., and Beucke, K. E., 1983, "A Frictional Damped Base Isolation System with Fail-Safe Characteristics," *Earthquake Engineering and Structural Dynamics,* Vol. 11, pp. 33–56.

Lin, B. C., Tadjbakhsh, I. G., Papageorgiou, A. S., and Ahmadi, G., 1990, "Performance of Earthquake Isolation Systems," *Journal of Engineering Mechanics, ASCE,* Vol. 116, pp. 446–461.

Mostaghel, N., and Khodaverdian, M., 1987, "Dynamics of Resilient-Friction Base Isolator (R-FBI)," *Earthquake Engineering and Structural Dynamics,* Vol. 15, pp. 379–390.

Mostaghel, N., and Tanbakuchi, J., 1983, "Response of Sliding Structures to Earthquake Support Motion," *Earthquake Engineering and Structural Dynamics,* Vol. 11, pp. 355–366.

Su, L., Ahmadi, G., and Tadjbakhsh, I. G., 1989, "A Comparative Study of Base Isolation System," *Journal of Engineering Mechanics, ASCE,* Vol. 115, pp. 1976–1992.

Wen, Y. K., 1976, "Method for Random Vibration of Hysteretic Systems," *Journal of Engineering Mechanics, ASCE,* Vol. 102, pp. 249–263.